

Supporting Information

1

2 **Highly Conjugated Three-Dimensional van der Waals** 3 **Heterostructures Based Nanocomposite Films for Ultrahigh-** 4 **Responsivity TEA Gas Sensors at Room Temperature**

5 **Shaofeng Shao,^{a,b*} Chunyu Xie,^a Yuxuan Xia,^a Lei Zhang,^{a*} Jun Zhang,^{b,c} Song Wei,^a**
6 **Hyoun Woo Kim,^d and Sang Sub Kim^e**

7 ^a *Institute of Advanced Materials and Flexible Electronics (IAMFE), School of Chemistry and Materials*
8 *Science, Nanjing University of Information Science & Technology, 210044, Nanjing, China. Fax: +86-*
9 *025-58731031; Tel: +86-025-58731031; E-mail: ssfshao@nuist.edu.cn, ervin42772@gmail.com.*

10 ^b *Key Laboratory of Advanced Energy Materials Chemistry (Ministry of Education), Nankai University,*
11 *Tianjin 30071, China.*

12 ^c *College of Physics, Centre for Marine Observation and Communications, Qingdao University, Qingdao*
13 *266071, China.*

14 ^d *Division of Materials Science and Engineering, Hanyang University, Seoul 04763, Republic of Korea.*

15 ^e *Department of Materials Science and Engineering, Inha University, Incheon 22212, Republic of Korea.*

16 ***Corresponding authors:**

17 Shaofeng Shao, E-mail: ssfshao@nuist.edu.cn, Fax: +86-025-58731031, Tel: +86-025-58731031

18

1 **1. Experimental Section**

2 **1.1 Characterization**

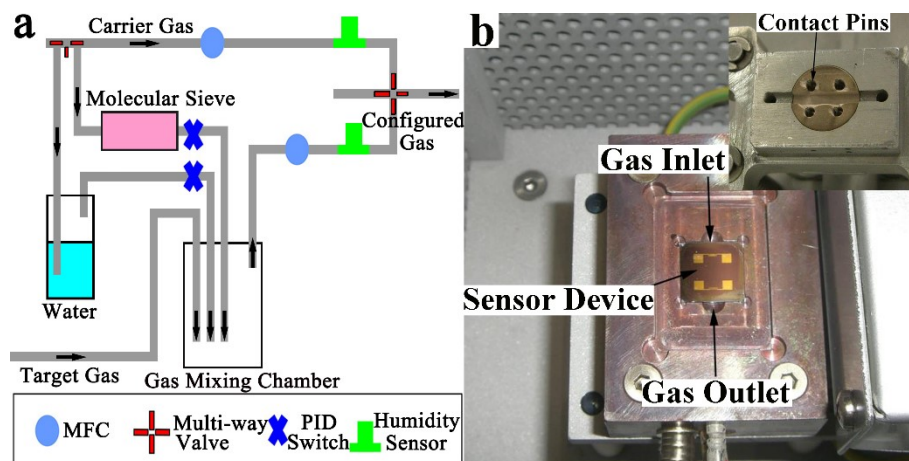
3 XRD analyses were conducted on a Rigaku Smartlab X-ray diffractometer with Cu
4 $K\alpha$ radiation. The morphology of the sensing materials was examined by a scanning electron
5 microscopy (FE-SEM, ZEISS, GeminiSEM 300) and a transmission electron microscope (an
6 FEI Titan 80-300 equipped with a field emission gun operated at 300 kV). XPS analysis was
7 performed using a Kratos Axis Ultra DLD spectrometer. Surface charging was corrected by
8 referencing the spectra to the C-C state of the C 1s peak at binding energy at 284.6 eV. All XPS
9 spectra were recorded using an aperture slot of 300*700 microns, survey spectra were recorded
10 with a pass energy of 160 eV, and the high-resolution spectra with a pass energy of 40 eV.
11 Nitrogen sorption measurements were carried out at 77 K using a Micromeritics ASAP2460
12 Instrument on sensing materials scratched from several films. The Fourier transform infrared
13 spectra (FTIR) of the samples were recorded on an AVATAR370FT-IR spectrophotometer
14 using conventional KBr pellets.

15 **1.2 Gas Sensor Measurement**

16 To identify the gas response characteristics of the sensors in the highly humid atmosphere, the
17 humidity level was maintained in the range of 50-90% RH in the testing sensor chamber by the
18 gas distribution system, as shown in Fig. S1a. Gas-sensing tests were performed at room
19 temperature against the 10 target gases at various concentrations (0.2-25 ppm) to evaluate the
20 gas-sensing performance of the nanocomposites. The high resistance meter Keithley 6517B
21 recorded resistance changes upon sample exposure to different gases. A certain concentration
22 of target gas is periodically passed into the test chamber based on computer-controlled mass
23 flow controllers (MFCs), and the total flow rate is maintained at 500 sccm. The gas sensing
24 properties were determined in the sample cell with gas inlet and gas outlet, as shown in Fig
25 S1b. The sample cell could ensure that the gas flow was restricted to the sensing area of the
26 substrate and there was a constant gas flow over interdigitated-finger arrays of the sensor
27 device.

28

29

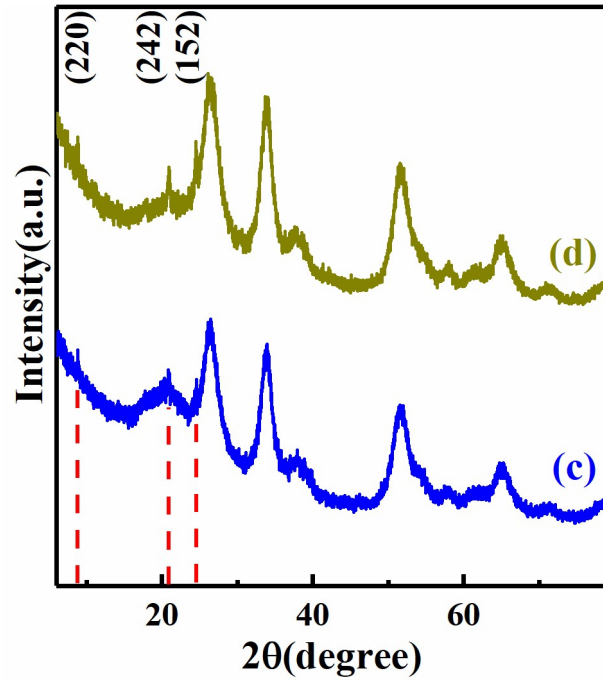


1
 2 **Fig. S1.** (a) The diagram of the gas distribution system. (b) The image of the sample chamber and sensor device.
 3 The insert image shows four contact pins for the sensor device. The sensor device obtains interdigitated-finger arrays
 4 and each finger is 10 μm in width and 1 mm in length. The finger-finger spacing is 8 μm , and with a finger-to-finger
 5 overlap of 800 μm .

	<i>CNC</i>	<i>SnO₂ QNP</i>	<i>Dip-coated COFs Precursor</i>	<i>VIST Treated in Ar</i>	<i>Doping Pt</i>	<i>Methanol- Vapour Treatment</i>	<i>Ar-Plasma Treatment</i>
<i>CSC1T</i>	✓	✓	Dip-coated one time	40 h	×	×	×
<i>CSC3T</i>	✓	✓	Dip-coated three times	40 h	×	×	×
<i>CSC5T</i>	✓	✓	Dip-coated five times	40 h	×	×	×
<i>PCSC1T</i>	✓	✓	Dip-coated one time	40 h	✓	24 h	×
<i>PCSC3T</i>	✓	✓	Dip-coated three times	40 h	✓	24 h	×
<i>PCSC5T</i>	✓	✓	Dip-coated five times	40 h	✓	24 h	×
<i>PCSC1T- P10m</i>	✓	✓	Dip-coated one time	40 h	✓	24 h	10 minutes
<i>PCSC3T- P2m</i>	✓	✓	Dip-coated three times	40 h	✓	24 h	2 minutes
<i>PCSC3T- P5m</i>	✓	✓	Dip-coated three times	40 h	✓	24 h	5 minutes
<i>PCSC3T- P10m</i>	✓	✓	Dip-coated three times	40 h	✓	24 h	10 minutes
<i>PCSC3T- P15m</i>	✓	✓	Dip-coated three times	40 h	✓	24 h	15 minutes
<i>PCSC5T- P10m</i>	✓	✓	Dip-coated five times	40 h	✓	24 h	10 minutes

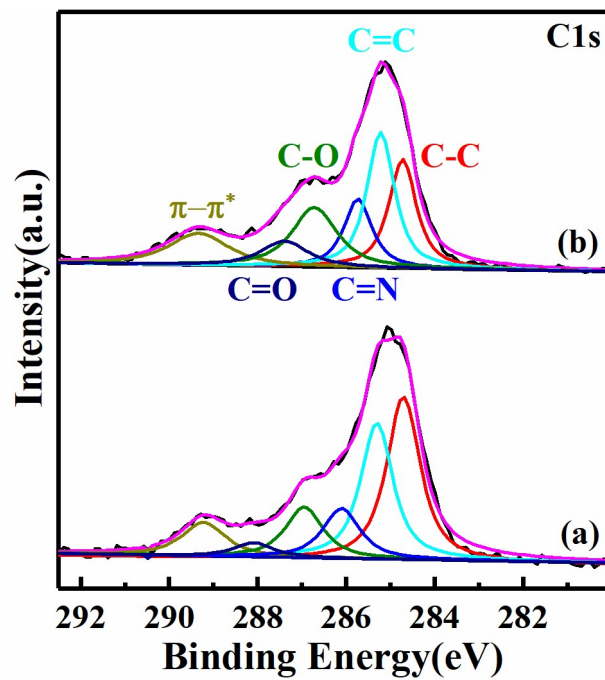
1

Table. S1. List of the synthesis process about different samples.



1

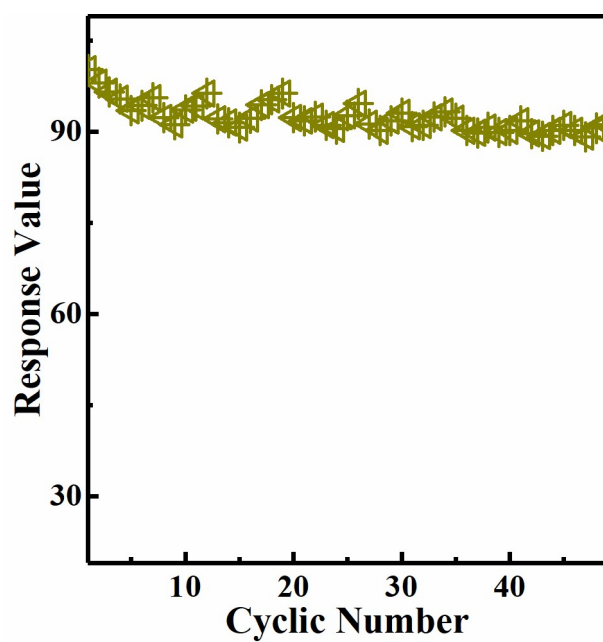
2 Fig. S2. WAXRD patterns of COFs@SnO₂QNP@CNS (c), and Pt@COFs@SnO₂QNP@CNS (d);



1
2
3

Fig. S3. The high-resolution XPS spectrum of C 1s of PCSC3T (a) and PCSC3T-P10m (b).

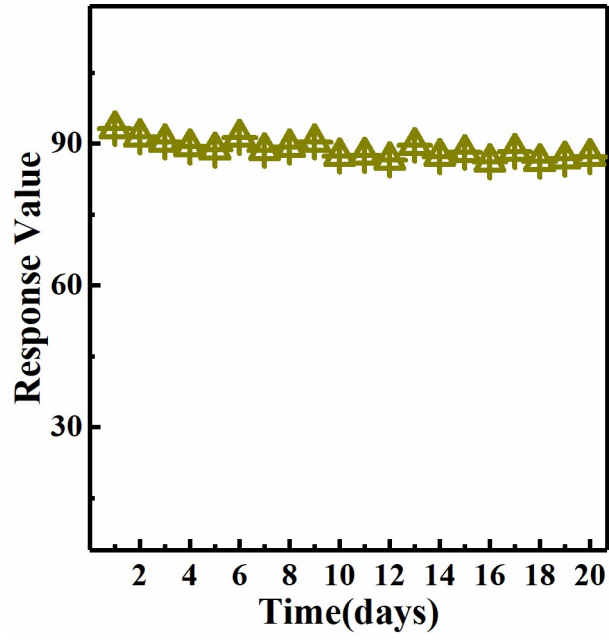
1



2

3 **Fig. S4.** Response of PCSC3T-P10m sensor to 2.0 ppm TEA as a function of the number of cyclic measurements.

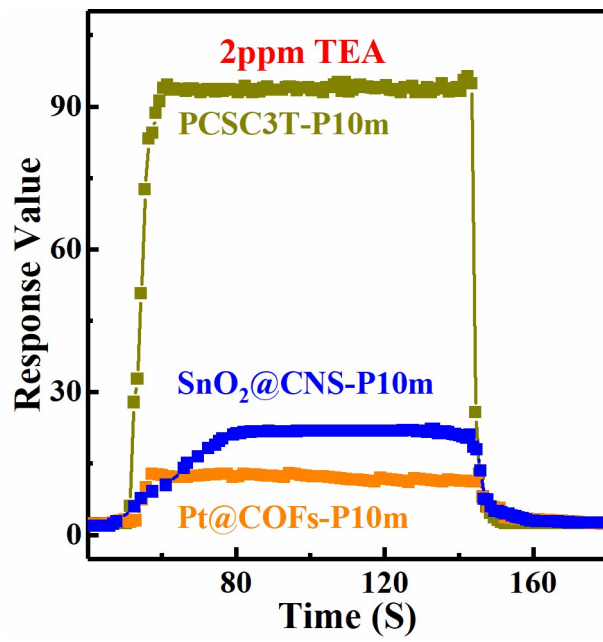
4



1

2 **Fig. S5.** Response stability of the sensors composed of PCSC3T-P10m to 2.0 ppm TEA gas, operated at room
3 temperature for almost 3 weeks. Minor changes are observed for the developed sensor, indicating acceptable long-
4 term stability in real applications.

5



1

2 Fig. S6. Response of PCSC3T-P10m, SnO₂@CNS-P10m, Pt@COFs-P10m to 2.0 ppm TEA at room temperature.

3